

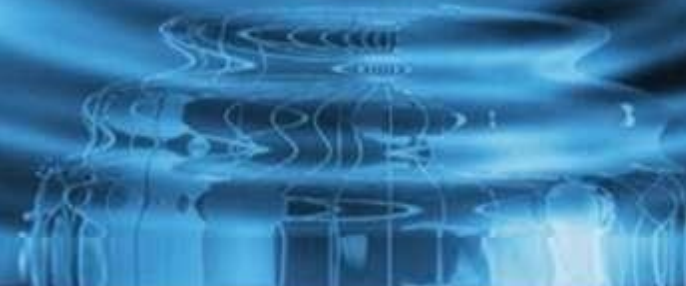


**IJITCE**

**ISSN 2347- 3657**

# **International Journal of Information Technology & Computer Engineering**

[www.ijitce.com](http://www.ijitce.com)



**Email : [ijitce.editor@gmail.com](mailto:ijitce.editor@gmail.com) or [editor@ijitce.com](mailto:editor@ijitce.com)**

# Computer simulation of shrinkage related defects in metal castings – a review

CH. CHARAN KUMAR

## Abstract

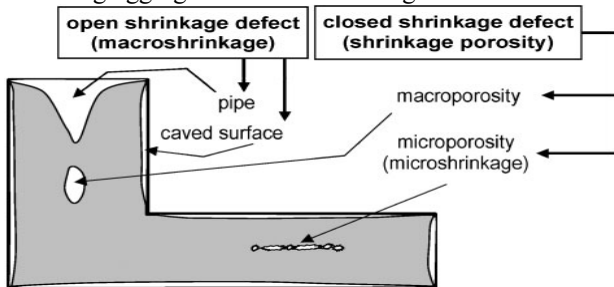
The possibility for shrinkage-related fault simulation in form castings to aid in the enhancement of cast product quality has prompted much research into the topic. It is currently challenging to measure the magnitude of macroshrinkage, even if its position may be calculated quite readily using contemporary solidification models. There have been many attempts and assertions of accomplishment, but microporosity prediction remains an unsolved mystery. Following a brief introduction to the underlying physics, this paper goes on to discuss the different methods used to model the evolution of macro- and micro-porosity. These methods range from basic thermal models and criterion functions to more advanced models based on oxide entrapment, channel and porous medium, and hydrogen diffusion, respectively.

**Keywords:** Computer simulation; Shrinkage defects; Porosity; Thermal modelling; Criterion functions

## INTRODUCTION

Shrinkage porosities and shrinkage cavities are two types of flaws caused by the solidification of the casting, which occurs when the liquid metal interacts with the moulding aggregate. As a result of high rework costs or

casting rejection, these flaws have a detrimental economic effect on casting production. All these problems' occurrences may be explained inside the mushy zone in relation to metal flow



### 1 The term "shrinkage defect" and its categorization

In order to fill the mass deficit caused by solidification shrinkage, the uninterrupted flow of liquid metal to the solidifying zone is crucial to the casting's soundness. Defects in shrinkage will occur if the mass deficit is not fed. Due to the vagueness of the nomenclature, this research will make use of the categorization and definitions given in Figure 1. Metal contracts both as it cools from a liquid condition and when it solidifies, leaving behind imperfections that are exposed to the environment; these are known as shrinkage voids. A procedure that does not rely on the metal's gas content and does not need the nucleation and expansion of gas pores is the use of atmospheric gases to make up for the mass deficit caused by shrinking. Closed shrinkage flaws, in contrast, appear to be concentration- and gas-dependent, since they are correlated with mushy zone

pore nucleation and growth. So, although metal contraction (shrinkage flow) is the primary driver of shrinkage cavities, pore nucleation and growth are the primary drivers of shrinkage porosity. Another possible consideration is mold deformation. Nearly always, when macroshrinkage is unrestricted the riser rejects the casting. While porosity isn't always a cause to throw out the casting, it does affect mechanical qualities including ductility, dynamic properties, fatigue life, and dynamic properties adversely. The influence of porosity on fracture initiation causes fatigue life to decrease as the maximum pore size increases (Fig. 2), as shown by Boileau and Allison<sup>5</sup>, who corroborated previous studies. Pore size is inversely proportional to both the local solidification time and the SDAS. Hot isostatic pressing (HIP) significantly increases fatigue life by eliminating porosity.

## The physics of defect formation

### Open shrinkage defects

1 Pipe formation is the direct result of the mass deficit produced by metal contraction. The solidification front must be continuously fed with liquid metal to avoid macroshrinkage formation. The feeding ability of the liquid decreases continuously as the metal solidifies. Before the beginning of solidification, liquid feeding occurs unimpeded. When solidification starts, solid grains form in the liquid. As long as these grains Relationship between pore size and fatigue life for Al alloy W319-T7 (alternating stress of 96.5 MPa)<sup>5</sup>

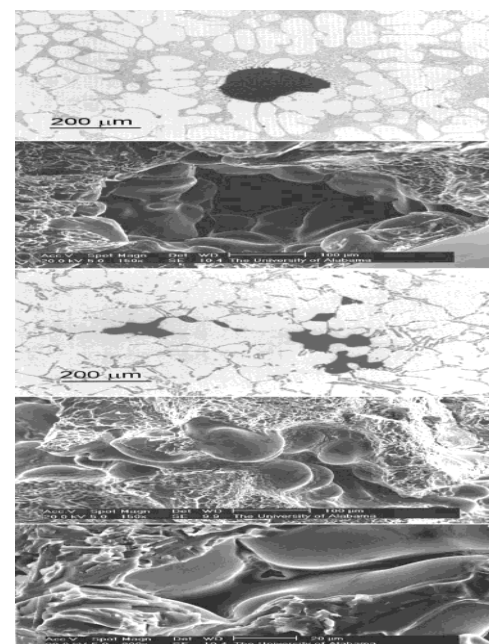
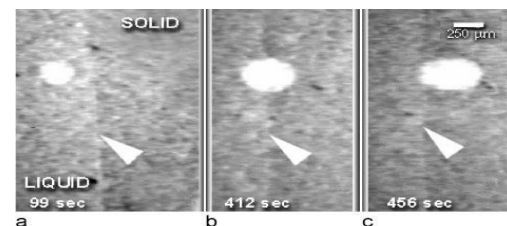
are not in contact with one another, i.e. when the fraction solid is smaller than the fraction solid corresponding to coherency, it may be assumed that the solid moves with the liquid and the alloy behaves like a slurry. Its relative viscosity is increased, causing the flow velocity to decrease during semisolid feeding. As solidification proceeds, dendrite coherency occurs and a fixed solid network forms. A further decrease in feeding occurs. Only interdendritic feeding is possible at this point.<sup>6</sup>

It has been suggested that the dendritic network collapses during solidification, causing a redistribution of liquid and solid, which has been termed burst feeding.<sup>7</sup> Recent research by Dahle *et al.*<sup>8,9</sup> seems to confirm this hypothesis. Indeed, their measurements suggest that interdendritic fluid flow can develop stresses in the mushy region that are of the same order of magnitude as the shear strength of the interdendritic network.

Once solidification is complete, only limited solid feeding through elastic and plastic deformation of the alloy is possible. This is responsible in part for the formation of caved surfaces.

Pipe shrinkage is common in all alloys. Wide mushy zone alloys can allow deformation of the mushy zone because of shrinkage, resulting in caved surfaces. In narrow mushy zone alloys that form a solid shell next to the mould early during solidification, the mass deficit can be accounted for in three ways: formation of closed shrinkage (macro- or micro-porosity) in the last region to solidify, plastic deformation of the solid shell resulting in caved surfaces, or formation of a large number of vacancies. Based on experimental evidence it is safe to assume that all three mechanisms are activated during solidification.

The driving forces for feeding are the metallostatic pressure and the negative shrinkage pressure developed during mushy zone solidification. However, since the defect is typically located in the proximity of the last region to solidify, early models were limited to finding this region. Nevertheless, from this analysis it is apparent that the accurate prediction of shrinkage cavity formation must be based on three phase (liquid, solid and gas) mass conservation, coupled



with energy conservation. To include casting

**3.**

Three real-time radiographs of the pure aluminum pore: one taken before the contact with the S/L, and two more taken after the interface with the S/L, showing the ellipsoidal evolution that occurs throughout the interaction. It is necessary to simulate deformation and stress as well. Stress analysis is often omitted from shrinkage models. Level of porosity While the liquid is cooling and solidifying, a considerable quantity of gas that has been dissolved is turned away by the formation of gas bubbles, which initiates porosity, when a certain pressure is exceeded in a liquid. When gas bubbles are created in a liquid, they float about until they encounter the solid/liquid (S/L) interface, where they finally create gas porosity. You can't call this a shrinking flaw. Gas trapped in dendrite network and microporosity or other localized shrinkage holes may occur if gas formation occurs in the mushy zone during late solidification, following dendrite coherency. little water loss. Porosity of gas A gaseous inclusion has a complicated interaction with the S/L interface. A planar S/L interface may encompass the gas pore at a specific interface velocity, according to recent work<sup>10</sup> on Al and Al-25Au. Even as it becomes engulfed, the pore keeps becoming bigger. When the pore is located distant from the S/L contact, the expansion of the pore is caused by hydrogen diffusion via the liquid phase, according to real-time observations of pore growth in pure Al. The rate of growth rises as the S/L contact gets closer to the pore. As seen in Figure 3, the pore now has a circular cross-section. When the solutal field, which is hydrogen, starts to interact with the pore before the S/L contact, the pore development rate increases dramatically. As the contact slowly surrounds the pore, its form changes to that of an ellipsoid. The solid will trap the pore if the contact is not flat. The form of the pore might be either elliptical (Fig. 4a,b) or spherical. Its dimensions could be on the micrometer to millimeter scale. This study will not address this flaw in any greater detail. Porous cracks The pore's form often mimics that of a dendritic rather than a sphere (Figs. 4c, d and 5). Microporosity is the name given to this flaw.

1 Microshrinkage in ductile iron (bottom image is enlargement of top one)<sup>13</sup>

or microshrinkage and can range in size from micrometres to hundreds of micrometres.

Not only the size but also the shape of the

microshrinkage is important. In well degassed melts, microshrinkage takes the shape of the interdendritic liquid that remains just before eutectic solidification (Fig. 4e) and the stress concentration factors resulting from these shapes are much higher than for spherical pores.<sup>14</sup>

The present understanding of microporosity formation is that metal flows toward the region where shrinkage is occurring until flow is blocked, either by solid metal or by a solid or gaseous 6. The mushy zone of ductile iron and its pressure and gas content force acting on the pore  $P_c$  due to surface tension in inclusion. Walther et al.<sup>15</sup> established the initial hypothesis was under the impression that flow stops coming in only when the cross-sectional area of the feeding channel continuously decreases during solidification. When the section of the channel has decreased too much the pressure drop ruptures the liquid in the channel forming a pore. However, pure liquids have high tensile strengths, capable of collapsing the surrounding solid and preventing fracture of the liquid.<sup>16</sup> It is implied that in the absence of gas pressure the tensile stress in the liquid will prevent any discontinuity formation.

More recent models assume that when a gas pore appears in the mushy zone in the later stages of solidification, after dendrite coherency, it is entrapped in the dendritic network. When the metal flow toward the solidification front is blocked, the pore becomes the starting point of microshrinkage. Thus, microshrinkage formation depends on the nucleation and growth of micropores. This concept can be understood from the analysis of the local pressure summarised in Fig. 6 for the case of ductile iron.  $P_{mush} \sim P_{appl} \geq P_{st} \geq P_{exp} \geq P_{shr}$

(1)

where  $P_{appl}$  is the applied pressure on the mould (e.g. atmospheric pressure),  $P_{st}$  is the metallostatic pressure,  $P_{exp}$  is the expansion pressure because of phase transformation and  $P_{shr}$  is the negative pressure from resistance to shrinkage induced flow through the fixed dendrite network. The equation can be rearranged to highlight the driving force on the left hand side

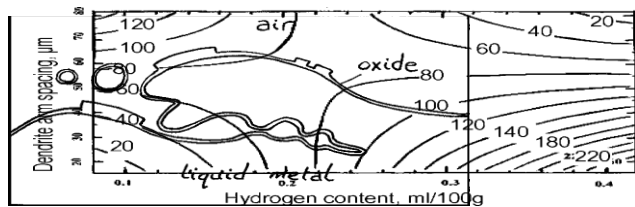
$$P_G \geq P_{shr} > P_{appl} \geq P_{st} \geq P_{exp} \geq P_c : : : : (2)$$

This equation shows that the driving forces for pore occurrence are the gas and shrinkage pressures. If the metal is completely degassed the shrinkage

pressure must reach the level of the shear stress of liquid metal for a vacuum pore to occur. Pore nucleation can occur when the gas dissolved in the liquid  $C_L$  exceeds the maximum solubility in the liquid  $C^{\max}$  (Fig. 6). The stability of such a pore is controlled by the surface energy pressure on the gas pore. Its mathematical expression is given

by Mathematically this is expressed through a pressurebalance equation stating that the pressure exerted by

mould filling. Oxide films may fold and produce bifilms (Fig. 8). If the liquid is assumed to be full of bifilms (i.e. cracks) the liquid has the potential to



2 Effect of gas content on dendrite arm spacing and on number of pores per square cm (Ref. 20)

nucleation of a pore in the liquid is unlikely since  $P_c$  is immense at the very small initial radius of the pore. Experimental evidence suggests that gas pores nucleate heterogeneously on inclusions that are present in the melt.<sup>17-19</sup> This could explain why filtering molten aluminium alloys reduces porosity in castings.

In the case of ductile iron, eutectic graphite produces a positive expansion pressure  $P_{\text{exp}}$  which counteracts the shrinkage and gas pressure. If the expansion pressure equals or exceeds the shrinkage pressure, porosity is completely avoided. However, this requires a completely rigid mould which is rarely the case in practice. Note that since  $P_{\text{shr}}$  is a direct function of the solidification shrinkage, the expansion pressure could be treated mathematically as a negative shrinkage pressure.

Microshrinkage is a major defect in Al-Si alloys because of the hydrogen dissolved in the liquid. It is generally accepted that the amount of microshrinkage decreases with the amount of hydrogen dissolved in the melt. Yet, this is not always the case. As shown in Fig. 7, work on small tapered plates and end chilled plates of Al-7Si-0.4Mg found that at short solidification times the pore density rose with increasing hydrogen content.

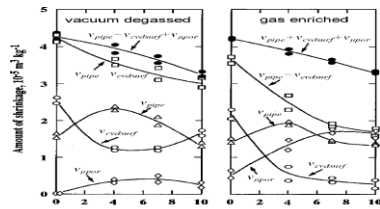
However, at long solidification times the pore density fell as hydrogen content increased.<sup>20</sup>

According to Campbell,<sup>21</sup> this apparently confusing effect can be explained if it is accepted that pore nucleation occurs inside oxide films as thin as 20 nm formed in liquid aluminium during

initiate pores with negligible difficulty. The biofilms simply open by the separation of their unbonded halves. Surface tension is not involved as assumed when nucleating a pore in a liquid.

Such a pore initiation mechanism can explain the data in Fig. 7 as follows. At low gas contents and short solidification times the biofilms remain folded

and porosity is minimal. As the solidification time (dendrite arm spacing) increases, at the same gas level, the biofilms start opening and gas porosity



increases. This is also true for high gas contents and low solidification times. At high gas contents and solidification times, large gas pores are formed, which decreases the area density of pores.

3 Recent research has demonstrated that the shrinkage defects at different length scale (macro and micro) Schematic view of surface turbulence, acting to fold in oxide film and bubbles<sup>21</sup>

interact with one another and must be understood together. A certain correlation seems to exist between the total amount of porosity, open shrinkage cavity and caved surface. Awano and Morimoto<sup>22</sup> who investigated the shrinkage behaviour of Al-Si alloys with various silicon and gas (vacuum degassed, non-treated, and gas enriched) contents, concluded that the total amount of shrinkage is constant at the same silicon level, but varies with the amount of gas in the melt. As summarised in Fig. 9, the total shrinkage depends little on the amount of gas, but decreases with higher silicon content. Microporosity, on the other hand, is a direct function of the gas content, as is further evident from Fig. 10.

Awano and Morimoto<sup>22</sup> further found that for alloys with a large solidification interval (mushy solidification), the amount of pipe is constant in the low porosity region (low to moderate gas content), but decreases with increasing porosity in the high porosity region (high gas content). For alloys that solidify with a small solidification interval (skin solidification), the amount of caved surface is constant in all porosity regions, while the amount of pipe decreases with increased porosity as the pore generation during the early

stage of solidification compensates for shrinkage.

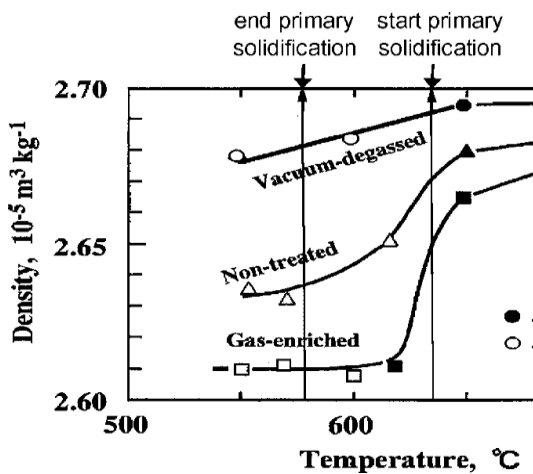
Effect of Si content on amount of shrinkage defects in Al-Si alloys ( $V_{\text{pipe}}$  is volume of pipe,  $V_{\text{cavsurf}}$  is volume o

cooling rate, solidification velocity, thermal gradient, etc.) to the shrinkage defect susceptibility. These models will be reviewed in some detail below.

Depending on the assumptions on the physics of the problem and the mathematical apparatus used the different approaches to shrinkage defect prediction can be summarised as follows (see also reviews in Refs. 6, 12, 23):

- (i) thermal models: solve energy transport equations to identify the last region to solidify or regions where feeding becomes restricted
- (ii) thermal/volume calculation models: solve energy transport equations and mass conservation to predict the position of the free surface and of the last region to solidify
- (iii) thermal/fluid flow models: solve mass and energy transport equations to predict the position of the free surface and of the last region to solidify
- (iv) transport/stress analysis models  
nucleation and growth of gas pores models: compute pore nucleation and growth when introducing a shrinkage ratio that is a function of temperature (see for example Ref. 30), Suri and Paul<sup>33</sup>

caved surface and  $v_{\text{por}}$  is volume of microporosity)



#### 4 Correlation between microporosity and hydrogen content in two Al-Si alloys<sup>22</sup>

Quenching experiments on an Al-4Si alloy<sup>22</sup> demonstrated that most of the pores are formed immediately after the start of primary solidification (Fig. 11).

This analysis reveals the complexity of the problem. Computational modelling of microshrinkage formation must describe phenomena such as porosity nucleation and growth, elastic and plastic deformation of the solidification shell and interdendritic flow.

**Approaches to modelling of shrinkage defects** From the previous analysis it becomes clear that the prediction of the location and size of shrinkage related defects is a difficult task. There have been numerous attempts at answering the problem through complex numerical 3D models that solve the transport equations. However, the mathematical complexity of these models and the lack of reliable databases have led a number of investigators to develop simpler analytical equations termed 'criterion functions' to predict when and where there is a high probability of defect formation in a casting. Criterion functions are simple rules that relate the local conditions (e.g.

## Thermal / volume calculation models

These models solve the heat transport problem and attempt to predict defect locations through simple change in volume calculations based on mass conservation, thus avoiding rigorous flow analysis of the molten metal during solidification. Imafuku and Chijiwa<sup>31</sup> were the first to propose such a model for prediction of the shape of macroshrinkage in steel sand castings. The main assumptions of the model are:

- (i) gravity feeding occurs instantly (liquid metal moves only under the effect of gravity, solidification velocity is much smaller than flow velocity)
- (ii) liquid metal free surface is flat and normal to the gravity vector
- (iii) the volume of shrinkage cavity is equal to the volume contraction of the metal
- (iv) macroscopic fluid flow exists as long as the fraction solid  $f_s$  is less than a critical fraction of 0.67.

The net change in volume because of shrinkage is calculated with

**Note on dimensionality of criterion functions** Most of the criteria presented in this paper are size (scale) and shape dependent. Very few are scale and shape independent. For example, Pellini's criterion is size dependent. Niyama's criterion is scale independent but shape dependent. However, the Hansen-Sahm criterion is scale and shape independent.

Hansen *et al.*<sup>73</sup> have demonstrated that scaling relationships should satisfy the condition  $C \sim C_0 N^m$

## References

1. S. Z. URAM, M. C. FLEMINGS and H. F. TAYLOR: *Trans. AFS*, 1958, 66, 129.
2. A. M. SAMUEL and F. H. SAMUEL: *Metall. Mater. Trans. A*, 1999, 26A, 2359.
3. B. SKALLERUD, T. IVELAND and G. HARKEGARD: *Eng. Fract. Mech.*, 1993, 44, 857.
4. J. F. MAJOR: *Trans. AFS*, 1997, 105, 901.
5. J. M. BOILEAU and J. E. ALLISON: *Metall. Mater. Trans. A*, 2003, 34A, 1807.
6. D. M. STEFANESCU: 'Science and engineering of casting solidification'; 2002, New York, Kluwer Academic / Plenum Publishers.
7. J. CAMPBELL: *AFS Cast Met. Res. J.*, March, 1969, 1.
8. R. POIRIER, K. YEUM and A. L. MAPLES: *Metall. Trans. A*, 1987, 'Solidification and materials processing', (ed. R. Abbaschian *et al.*), 363; 2003, Warrendale, PA, TMS.
9. R. RUXANDA, L. BELTRAN-SANCHEZ, J. MASSONE and D. M. STEFANESCU: *Trans. AFS*, 2001, 109, 1037.
10. J. T. BERRY: *Trans. AFS*, 1995, 103, 837.
11. W. D. WALTHER, C. M. ADAMS and H. F. TAYLOR: *Trans. AFS*, 1956, 64, 658.
12. J. CAMPBELL: 'Casting'; 1991, Oxford, UK, Butterworth Heinmann.
13. E. J. WHITENBERGER and F. N. RHINES: *J. Met.*, April, 1952, 409.
14. N. ROY, A. M. SAMUEL and F. H. SAMUEL: *Metall. Mater. Trans. A*, 1996, 27A, 415.
15. P. S. MOHANTY, F. H. SAMUEL and J. E. GRUZLESKI: *Trans. AFS*, 1995, 103, 555.
16. K. TYNELIUS, J. F. MAJOR and D. APELIAN: *Trans. AFS*, 1993, 101, 401.
17. J. CAMPBELL: in 'Modelling of casting, welding and advanced solidification processes X', (ed. D. M. Stefanescu *et al.*), 209; 2003, Warrendale, PA, TMS.
18. Y. AWANO and K. MORIMOTO: *Int. J. Cast Met. Res.*, 2004, 17, 107.
19. P. D. LEE, A. CHIRAZI and D. SEE: *J. Light Met.*, 2001, 1, 15.
20. J. G. HENZEL and J. KEVERIAN: *J. Met.*, 1965, 17, 561.
21. N. CHVORINOV: *Giesserei*, 1940, 27, 201.
22. G. K. UPADHYA and A. J. PAUL: *Trans. AFS*, 1992, 100, 925.
23. V. SURI and K. O. YU: in 'Modelling for casting and solidification processing', (ed. K. O. Yu), 95; 2002, New York, Marcel Dekker Inc.
24. W. S. PELLINI: *Trans. AFS*, 1953, 61, 61.
25. G. K. SIGWORTH and C. WANG: *Metall. Trans. B*, 1993, 24B, 365.
26. Y. W. LEE, E. CHANG and C. F. CHIEU: *Metall. Trans. B*, 1990, 21B, 715.
27. I. IMAFUKU and K. CHIJIWA: *Trans. AFS*, 1983, 91, 527.
28. R. HUMMER: *Cast Met.*, 1988, 1, 62.
29. V. K. SURI and A. J. PAUL: *Trans. AFS*, 1993, 144, 949.
30. J. BEECH, M. BARKHADAROV, K. CHANG and S. B. CHIN: in 'Modelling of casting, welding and advanced solidification processes VII', (ed. B. G. Thomas and C. Beckerman), 1071; 1998, Warrendale, PA, TMS.
31. L. I. JIARONG, B. LIU, H. XIANG, H. TONG and Y. XIE: Proc. '61st World Foundry Congress', Beijing, China, 1995, International Academic Publishers, 41.
32. T. S. PIWONKA and M. C. FLEMINGS: *Trans. AIME*, 1966, 236, 1157.
33. E. NIYAMA, T. UCHIDA, M. MORIKAWA and S. SAITO: *AFS Cast Met. Res. J.*, 1982, 7, 52.
34. J. A. SPITTLE, M. ALMESHEDANI and S. G. R. BROWN: *Cast Met.*, 1995, 7, 51.
35. H. HUANG, V. K. SURI, N. EL-KADDAH and J. T. BERRY: in 'Modelling of casting, welding and advanced solidification processes VI', (ed. T. S. Piwonka *et al.*), 219; 1993, Warrendale, PA, TMS.
36. V. K. SURI, A. J. PAUL, N. EL-KADDAH and J. T. BERRY: *Trans. AFS*, 1994, 138